Polymer 49 (2008) 4723–4732

Contents lists available at ScienceDirect

Polymer

journal homepage: www.elsevier.com/locate/polymer

Wound-dressing materials with antibacterial activity from electrospun gelatin fiber mats containing silver nanoparticles

Pim-on Rujitanaroj [a], Nuttaporn Pimpha [b], Pitt Supaphol [a,*]

[a] Technological Center for Electrospun Fibers and The Petroleum and Petrochemical College, Chulalongkorn University, Pathumwan, Bangkok 10330, Thailand
[b] National Nanotechnology Center, Thailand Science Park, Phathum Thani 12120, Thailand

ARTICLE INFO

Article history:
Received 1 July 2008
Received in revised form 2 August 2008
Accepted 6 August 2008
Available online 16 August 2008

Keywords:
Electrospinning
Fibrous membrane
Ag nanoparticles

ABSTRACT

Ultrafine gelatin fiber mats with antibacterial activity against some common bacteria found on burn wounds were prepared from a gelatin solution (22%w/v in 70 vol% acetic acid) containing 2.5 wt% $AgNO_3$. Silver nanoparticles (nAg), a potent antibacterial agent, first appeared in the $AgNO_3$-containing gelatin solution after it had been aged for at least 12 h, with the amount of nAg increasing with increasing aging time. The average diameters of the as-formed nAg ranged between 11 and 20 nm. Electrospinning of both the base and the 12 h-aged $AgNO_3$-containing gelatin solutions resulted in the formation of smooth fibers, with average diameters of ~230 and ~280 nm, respectively. The average diameter of the as-formed nAg in the electrospun fibers from the 12 h-aged $AgNO_3$-containing gelatin solution was ~13 nm. The nAg-containing gelatin fiber mats were further cross-linked with moist glutaraldehyde vapor to improve their stability in an aqueous medium. Both the weight loss and the water retention of the nAg-containing gelatin fiber mats in acetate buffer (pH 5.5), distilled water (pH 6.9) or simulated body fluid (SBF; pH 7.4) decreased with increasing cross-linking time. The release of Ag^+ ions from both the 1- and 3 h-cross-linked nAg-containing gelatin fiber mats – by the total immersion method in acetate buffer and distilled water (both at a skin temperature of 32 °C) – occurred rapidly during the first 60 min, and increased gradually afterwards; while that in SBF (at the physiological temperature of 37 °C) occurred more gradually over the testing period. Lastly, the antibacterial activity of these materials, regardless of the sample types, was greatest against *Pseudomonas aeroginosa*, followed by *Staphylococcus aureus*, *Escherichia coli*, and methicillin-resistant *S. aureus*, respectively.

1. Introduction

Electrospinning (e-spinning) is a process capable of producing fibers from materials of diverse origins, including polymers, with diameters in the nano- to micrometer range [1]. A polymer liquid (i.e., melt or solution) is first loaded into a container with a small opening (used as the nozzle), and is then charged with a high electrical potential across a finite distance between the nozzle and a grounded collection device. When the electric field increases beyond a critical value – at which the repulsive electrical forces overcome the surface tension of the polymeric liquid droplet at the tip of the nozzle – a charged jet is ejected [1]. As the jet travels to the collector, it either cools down (in case of the melt) or the solvent evaporates (in case of the solution) to obtain ultrafine fibers in the form of a non-woven fabric on the collector. The morphology of the electrospun (e-spun) fibers depends on a number of factors, such as solution properties (e.g., concentration, viscosity, conductivity, surface tension, etc.), processing conditions (e.g., electrical potential, collection distance, etc.), and ambient conditions (e.g., temperature, humidity, etc.) [2,3]. Some potential uses of e-spun fibers in biomedical fields are, for example, immobilization of enzymes [4], tissue-engineered scaffolds [5,6], and delivery carriers for DNA [7] and drugs [8–12].

Due to its natural abundance and inherent biodegradability in physiological environments, gelatin is widely used in food, cosmetic, pharmaceutical and medical applications [13]. Depending on its usage, gelatin can be fabricated in many forms, e.g., films [14], micro- or nanoparticles [15,16], and dense or porous hydrogels [17–19]. Gelatin in the form of micro- and nanofibers can also be fabricated by gel and e-spinning techniques, respectively [20–27]. Owing to the uniqueness of the e-spun fibers (e.g., high surface area to mass or volume ratio; high porosity of the e-spun fiber mat; and flexibility for surface functionalization), e-spun gelatin fibers are of interest here. Suitable solvents for preparing an electrospinnable gelatin solution are 2,2,2-trifluoroethanol (TFE) [21,22], formic acid [23,27], 1,1,1,3,3,3-hexafluoro-2-propanol (HFP) [24,25], and acetic acid [26,27]. The average diameters of the obtained e-spun gelatin fibers were 100–1900 nm (type-A gelatin; 5–15% w/v in TFE) [21];

* Corresponding author. Tel.: +66 2218 4131; fax: +66 2215 4459.
E-mail address: pitt.s@chula.ac.th (P. Supaphol).

0032-3861/$ – see front matter © 2008 Elsevier Ltd. All rights reserved.
doi:10.1016/j.polymer.2008.08.021

70–170 nm (type-A gelatin; 7–12 wt% in 98% formic acid) [23]; 80–490 nm (type-B gelatin; 2–8.3%w/v in HFP) [24]; 800 nm (type-B gelatin; 8% w/v in HFP) [25]; 210–840 nm (type-A gelatin; 15–29% w/v in glacial acetic acid) [26]; and 160–760 nm or 110–300 nm (extracted gelatin from Nile tilapia skin; 14–29% w/v in 40% v/v acetic acid or in 80% v/v formic acid, respectively) [27]. To improve their stability in an aqueous medium, e-spun gelatin fibers can be cross-linked by hexamethylene diisocyanate [24], 1-ethyl-3-(3-dimethylaminopropyl)-carbodiimide [25], or glutaraldehyde (GTA) vapor [27,28].

Because of the inherent properties of gelatin and the unique characteristics of the e-spun fibers, e-spun gelatin fibers are ideal materials to be used as scaffolds for cell and tissue culture [22,24,25], carriers for topical/transdermal delivery of drugs [29], and wound dressings. Dressings play a major role in modern management of certain types of open wounds (e.g., traumatic, thermal, or chronic wounds), since the moist, warm and nutritious environment of wound beds provides an ideal condition for microbial growth [30–33]. Bacterial colonization and subsequent infection can interfere with the wound healing process by producing various substances (e.g., toxins, proteases and pro-inflammatory molecules) which may cause an excessive and prolonged inflammatory response of the host tissues [30–33]. Ideal antimicrobial dressings should have a number of key attributes, including provision of a moist environment to enhance healing [34], and broad-spectrum antimicrobial activity, including activity against antibiotic-resistant bacteria [e.g., methicillin-resistant *Staphylococcus aureus* (MRSA)] [30–33]. A recent resurgence of the use of silver-based dressings has been ascribed to their broad-spectrum antibacterial activity, as well as to a lesser possibility for inducing bacterial resistance than antibiotics [31,32].

Here, e-spun gelatin fiber mats containing silver nanoparticles (hereafter, nAg) are proposed to be used as antibacterial dressings. Historically, a number of polymer-based materials have been fabricated into e-spun fibers containing nAg. These are polyacrylonitrile (PAN) [35,36], PAN/titanium(IV) oxide composite (TiO_2) [37], cellulose acetate (CA) [38,39], poly(*N*-vinylpyrrolidone) (PVP) [40], and poly(vinyl alcohol) (PVA) [40–42]. Yang et al. [35] prepared e-spun PAN fibers (~400 nm) containing nAg (~100 nm) from a PAN solution in *N*,*N*-dimethylformamide (DMF) using hydrazinium hydroxide as a reducing agent; while Lee et al. [36] prepared e-spun PAN fibers (~200 to 360 nm) containing nAg (<5.8 nm) from 7 wt% PAN solution containing silver nitrate ($AgNO_3$) at 0.05–0.5% by weight of PAN in DMF, with DMF also being used as a reducing agent. Lim et al. [37] showed that nAg (~2 nm) could be prepared by photocatalytic reduction with UV irradiation onto TiO_2 nanoparticles in e-spun PAN fibers from 10 wt% PAN solution in DMF. Photoreduction with UV irradiation was used to prepare e-spun cellulose acetate fibers (~610 to 680 nm) containing nAg (~3 to 21 nm) on their surfaces from 10 wt% CA solution in 80:20 v/v acetone/water containing $AgNO_3$ at 0.05–0.5% by weight of CA [38,39]. DMF was used to reduce silver ions (Ag^+) into nAg (~3.4 to 6.0 nm) in the preparation of e-spun PVP and PVA fibers from 47 wt% PVP solution in DMF containing $AgNO_3$ at 0.5% by weight of PVP; or from 12 wt% PVA aqueous solution containing 5 wt% of 47 wt% PVP solution in DMF containing $AgNO_3$ at 15% by weight of PVP, respectively [40]. Lastly, heat treatment and photoreduction with UV irradiation was used to prepare e-spun PVA fibers containing nAg (~5.9 to 107 nm) from 10 wt% PVA aqueous solution containing $AgNO_3$ at 0.1% by weight of PVA [41,42]. Some of these nAg-loaded e-spun fiber mats were tested for their antibacterial activity against *Escherichia coli*, *Klebsiella pneumoniae*, *Pseudomonas aeruginosa* and *S. aureus* [38,39,41,42].

In the present study, mats of gelatin fibers containing nAg were prepared by e-spinning. The proposed use of these e-spun fiber mats is as wound dressing pads. GTA vapor was used to improve the stability of the fiber mats in a moist environment. The nAg-containing gelatin fiber mats were characterized for release characteristics of the as-loaded silver, as well as for their antibacterial activity against some common bacteria found on burn wounds.

2. Experimental details

2.1. Materials

Gelatin powder (type A; porcine skin; 170-190 Bloom) was purchased from Fluka (Switzerland). Silver nitrate ($AgNO_3$; 99.998% purity) was purchased from Fisher Scientific (USA). Glacial acetic acid was purchased from Mallinckrodt Chemicals (USA). An aqueous solution of glutaraldehyde (GTA; 5.6 M or 50 vol%) was purchased from Fluka (Switzerland). All chemicals were of analytical reagent grade and used without further purification.

2.2. Preparation and characterization of gelatin solutions containing nAg

$AgNO_3$ was first dissolved in a quantity of 70:30 v/v glacial acetic acid/distilled water. A metered weight of gelatin powder was then added into the as-prepared $AgNO_3$ solution. Slight stirring was used to expedite the dissolution and homogenize the solution. The concentration of the base gelatin solution was 22% w/v (based on the volume of the mixed solvent), and the amount of $AgNO_3$ was 2.5% w/w (based on the weight of the gelatin powder). To investigate the effect of aging time on the formation of nAg, the $AgNO_3$-containing gelatin solution was aged in an amber glass bottle while being stirred for a varying period of time. Some of the aged $AgNO_3$-containing gelatin solutions were characterized for shear viscosity and conductivity using a Brookfield DV-III programmable rheometer and a SUNTEX SC-170 conductivity meter. The existence of the as-formed nAg in the as-aged $AgNO_3$-containing gelatin solutions was confirmed by monitoring the surface plasmon absorption band using a Shimadzu UV-2550 UV–visible spectrophotometer. The diameters of the as-formed nAg at various aging time points were examined by a Seiko SPA 400, SPI 4000 atomic force microscope (AFM). Specifically, a small drop from each nAg-containing gelatin solution was deposited on a freshly-cleaved mica substrate. Measurement was then performed on dried samples using a gold-coated silicon NSG 10 cantilever probe with 190–325 kHz resonance frequency in the tapping mode. All AFM images were recorded in air at room temperature at a scan speed of 1 Hz.

2.3. Preparation of neat and nAg-containing e-spun gelatin fiber mats

2.3.1. e-Spinning

The base gelatin solution and the $AgNO_3$-containing gelatin solution that had been aged for 12 h were fabricated into fiber mats by e-spinning. Firstly, each of the as-prepared solutions was loaded into a standard 10-mL glass syringe, the open end of which was attached to a blunt 20-gauge stainless steel hypodermic needle (OD = 0.91 mm), which was used as the nozzle. Both the syringe and the needle were tilted ~45 °C from a horizontal baseline. A piece of aluminum (Al) sheet wrapped around a rotating cylinder (OD and width ≈ 15 cm; ~40–50 rpm) was used as the collection device. A Gamma High-Voltage Research ES30P-5 W DC power supply (Florida, USA) was used to charge the solution by attaching the emitting electrode of positive polarity to the nozzle, and the grounding one to the collecting device. An electrical potential of 15 kV was applied across a distance of 20 cm between the tip of the needle and the outer surface of the collection device (i.e., collection distance, measured at a right angle to the surface of the collection

device). The e-spun fiber mats were collected continuously for 48 h. The thicknesses of the neat and the nAg-containing gelatin fiber mats were measured by a Mitutoyo digital micrometer to be 380 ± 50 and 390 ± 90 μm, respectively.

2.3.2. Cross-linking

Cross-linking of both the neat and the nAg-containing gelatin fiber mats was carried out by clamping each of the fiber mat samples between a pair of supporting stainless steel frames (4.5 cm × 10 cm) with adhesive tape. The clamped fiber mat samples were then placed into a sealed chamber saturated with the vapor from 20 mL of the as-received GTA aqueous solution. The temperature of the chamber was maintained at 37 °C, and each fiber mat sample was exposed to the moist GTA vapor for 1 or 3 h. After exposure, the samples were heat-treated in an oven at 110 °C for 24 h to enhance the cross-linking reaction and to remove most, if not all, of the unreacted GTA.

To assess the extent of cross-linking, specimens from both the neat and the nAg-containing gelatin fiber mat samples (circular discs ~1.5 cm in diameter) were weighed and then submerged in acetate buffer aqueous solution (pH 5.5) or distilled water (pH 6.9) – both at the skin temperature of 32 °C – or simulated body fluid (SBF; pH 7.4) at the physiological temperature of 37 °C, all for various submersion time intervals. Procedures for the preparation of acetate buffer and SBF are given in Supplementary data. The weight loss and water retention of these specimens were determined according to the following equations:

$$\text{Weight loss}\ (\%) = \frac{M_i - M_d}{M_i} \times 100, \quad (1)$$

$$\text{Water retention}\ (\%) = \frac{M - M_d}{M_d} \times 100, \quad (2)$$

where M is the weight of each specimen after submersion in the medium at each submersion time point, M_d is the weight of the specimen in its dry state after submersion in the medium at each submersion time point, and M_i is the initial weight of the specimen in its dry state.

2.3.3. Characterization

The neat and the nAg-containing gelatin fiber mats were examined either qualitatively or quantitatively for the size and/or the amount of both the individual fibers and the as-formed nAg using a JEOL JSM-6400 scanning electron microscope (SEM), a JEOL JEM-2100 transmission electron microscope (TEM), and an Oxford 2000 energy dispersive X-ray (EDX) facility of a Phillips PW 2400 X-ray fluorescence spectroscope. The average diameters of both the fibers and the as-formed nAg were determined from SEM and TEM images, respectively, using a custom-code image analytical software. The thermal behavior of the e-spun fiber mat samples, with or without cross-linking, was examined by a Perkin–Elmer Pyris Diamond thermogravimetric/differential thermal analyzer (TG-DTA). Measurements were conducted over a temperature range of 25–800 °C, at a heating rate of 10 °C min^{-1} under nitrogen purge. Mechanical integrity of the e-spun fiber mat samples, with or without cross-linking, was evaluated by a Lloyd LRX universal testing machine with 500 N load cell and 20 mm min^{-1} crosshead speed at ambient conditions. The specimens were cut from the e-spun fiber mat samples (rectangular shape; 70 mm × 10 mm) [22]. At least 10 specimens for each sample type were tested.

2.3.4. Loading capacity and release characteristic of as-loaded silver

Prior to the release assay, the actual amount of silver (either in the form of nAg or Ag^+ ions) in the uncross-linked nAg-containing gelatin fiber mat specimens (circular disc; 2.8 cm in diameter) and the form of silver (either nAg or Ag^+ ions) that was released from the specimens needed to be determined. The actual amount of silver was quantified by dissolving the specimens in 5 mL of 95% nitric acid (HNO_3), followed by the addition of a releasing medium (acetate buffer, distilled water, or SBF) to attain a total volume of 50 mL. After that, each of the silver-containing solutions was quantified for the amount of silver by a Varian SpectrAA-300 atomic absorption spectroscope (AAS). The results were reported as average values ($n = 3$). Additionally, the form of the released silver was examined by a titration technique using a Metter-Toledo T50 Version 1.1.0 titrator. The titration technique was used to verify whether silver in the form of ions (i.e., Ag^+) was released from the specimens. The measurements were carried out at room temperature (26 ± 1 °C) using Ag/AgCl electrode and 0.01 M NaCl aqueous solution as the titrant. About 50 mL of the sample solutions were prepared from 20 mL of the silver-containing releasing medium (either acetate buffer or distilled water) and 30 mL of distilled water, with the addition of 5 drops of 1 M HNO_3.

The release characteristics of silver from the nAg-containing gelatin fiber mats that had been exposed to the GTA vapor for 1 or 3 h was assessed in acetate buffer, distilled water, or SBF as the releasing medium. The specimens cut from the fiber mat samples (circular disc; 2.8 cm in diameter) were immersed in 50 mL of the releasing medium at the skin or physiological temperatures of 32 or 37 C, respectively, depending on the type of the releasing medium (i.e., 32 °C for both acetate buffer and distilled water, and 37 °C for SBF). At a specified immersion period ranging between 0 and 7 d, the releasing medium was quantified for the amount of released silver, using AAS. At each time point, the measurements were carried out in triplicate. The obtained data were carefully calculated to obtain the cumulative amount of released silver. The cumulative release profiles of silver were expressed based on either the unit weight of the specimens or the unit weight of the actual amount of silver in the specimens.

2.3.5. Antibacterial evaluation

The antibacterial activity of the e-spun fiber mats, both from the base gelatin solution and the 12 h-aged $AgNO_3$-containing gelatin solution – after having been cross-linked with moist GTA vapor for 1 or 3 h with or without glycine (0.1 M aqueous solution) washing – was tested against aerobic bacteria commonly found on burn wounds: e.g., *E. coli* (Gram-negative; ATCC 25922), *Pseudomonas aeroginosa* (Gram-negative; ATCC 27853), *S. aureus* (Gram-positive; ATCC 25023), and methicillin-resistant *S. aureus* (MRSA: Gram-positive; ATCC 20627). The assessment was conducted based on the disc diffusion method of the US Clinical and Laboratory Standards Institute (CLSI). Both the neat and the nAg-containing gelatin fiber mats were cut into circular discs (15 mm in diameter). Vancomycin was used as the control antibacterial drug for *S. aureus* and MRSA, while gentamicin was used for *E. coli* and *P. aeroginosa*. Each of the specimens and the control drugs were placed on Difco™ Mueller Hinton agar in a Petri dish, and then incubated at 37 °C for 24 h. If inhibitory concentrations were reached, there would be no growth of the microbes, which could be seen as a clear zone around the disc specimens. These were photographed for further evaluation.

3. Results and discussion

3.1. Formation of nAg in gelatin solutions and effect of aging time

A number of methods have been used to generate nAg from Ag^+ ions in e-spun fibers. They are: chemical reduction by hydrazinium hydroxide [35] or DMF [36,40]; photocatalytic reduction by TiO_2 nanoparticles [37]; photoreduction by UV irradiation [38,39,41,42]; and simple heat treatment [41,42]. In these, the as-formed nAg

were prevented from further growth and agglomeration (i.e., stabilized) by the polymer matrix [35,36,38–42]. Ag^+ ions were reduced directly into nAg through a series of steps, including nuclei formation, crystal growth via diffusion mechanism to give primary particles, and spontaneous self-organization of primary particles to form clusters (i.e., secondary particles) [43]. Here, the formation of the nAg nuclei was postulated to originate from ionic interactions between Ag^+ ions and either $-NH_2$ or –COOH groups, or both, on gelatin chains, according the following schemes:

$$H_2N{-}COOH + AgNO_3 \leftrightarrow H_2N{-}COOAg + HNO_3, \quad (1)$$

$$H_2N{-}COOH + AgNO_3 \leftrightarrow AgHN{-}COOH + HNO_3, \quad (2)$$

or from simple binding between Ag^+ ions and lone pair electrons of N and O atoms in the $-NH_2$ and –COOH groups [44], followed by the reduction of Ag^+ ions into nAg nuclei.

The reduction of Ag^+ ions into elemental Ag (i.e., nAg) in the $AgNO_3$-containing gelatin solutions at different aging times could be visualized from changes in the color of the solutions: from light yellow of the neat solution, to brown of the 1 d-aged $AgNO_3$-containing solution, to dark brown of the 10 d-aged $AgNO_3$-containing solution. Fig. 1 shows UV–visible absorption spectra of both the base gelatin solution and the $AgNO_3$-containing gelatin solutions that had been aged for various time intervals after preparation. No absorption of any kind was observed for the base gelatin solution. The surface plasmon absorption bands, centering around 420–430 nm, were first observed for the $AgNO_3$-containing gelatin solutions that had been aged for at least 12 h. Evidently an increase in the aging time resulted in the observed increase in the intensity of the bands, which gradually reached a plateau value at a long aging time (i.e., 10 d). This indicated that the number of Ag^+ ions that were converted into nAg increased with an increase in the aging time. It is postulated that, at 10 d of aging, almost all of the Ag^+ ions would be converted into nAg. Presumably, based on the relative constancy in the positions of the bands at different aging times, the average size of the nAg particles that were formed at different aging times was relatively the same. Fig. 2 shows an AFM image of the as-formed nAg in an $AgNO_3$-containing gelatin solution that had been aged for 6 d. Those obtained from the $AgNO_3$-containing gelatin solutions that had been aged for 1 and 3 d are reported as Supplementary data. The average diameters of these particles were found to range between 11 and 20 nm. According to existing reports in the literature, the relationship between the average diameter(s) of the as-formed nAg and the peak value(s) of the surface plasmon absorption band(s) can be summarized as follows [average diameter(s)/peak value(s)]: 100 nm/440 nm [35], 6.8 nm/416 nm [36], 3–21 nm/438–445 nm [39], and 3.4–6.0 nm/424 nm [40].

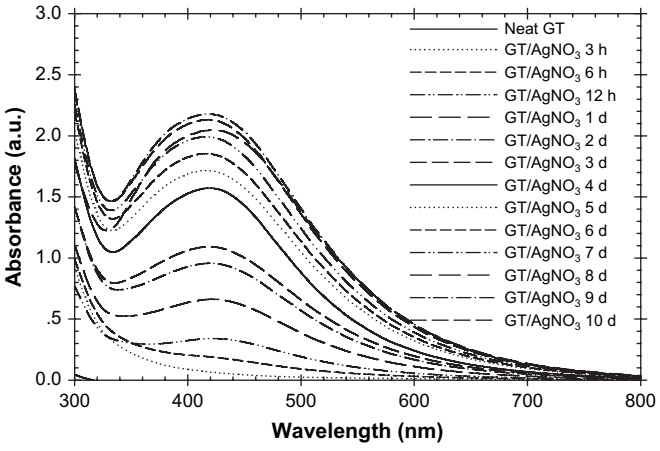

Fig. 1. Variation in UV–visible absorption spectra of the base gelatin (GT) solution and the $AgNO_3$-containing GT solutions that had been aged for different time intervals. The concentration of the base GT solution was 22 wt.% and the amount of $AgNO_3$ in the $AgNO_3$-containing GT solutions was 2.5 wt.% based on the weight of GT.

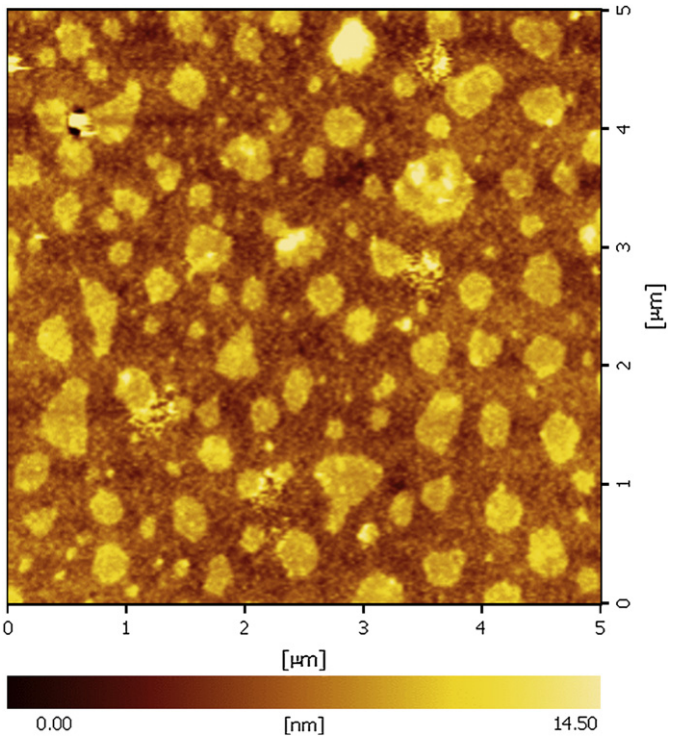

Fig. 2. AFM image of Ag nanoparticles (nAg) generated in the $AgNO_3$-containing gelatin solutions that had been aged for 6 d. The average diameter of these particles was 20 nm.

Prior to e-spinning, the base gelatin solution and some of the $AgNO_3$-containing gelatin solutions that had been aged for different time intervals were measured for their shear viscosity and conductivity. The results are summarized in Table 1. At a given aging time, the shear viscosity of the neat and the $AgNO_3$-containing gelatin solutions was essentially the same, while the conductivity of the $AgNO_3$-containing gelatin solution was greater than that of the base gelatin solution. This should be a result of the presence of Ag^+ and NO_3^- ions in the solution. For a given type of gelatin solution, a marked discrepancy in the property values was observed for the solutions that had been aged for 2 d. The observed decrease in the shear viscosity of the solutions that had been aged for 2 d should be a result of a considerable hydrolytic degradation of gelatin molecules [23].

Table 1
Shear viscosity and conductivity of the base gelatin (GT) and some of the $AgNO_3$-containing GT solutions that had been aged for different time intervals after preparation

Type of solution	Viscosity (cP)	Conductivity ($\mu S\,cm^{-1}$)
Base GT solution		
at 6 h	440 ± 1	1266 ± 1
at 12 h	441 ± 1	1270 ± 1
at 24 h	439 ± 1	1271 ± 2
at 2 d	363 ± 1	1199 ± 1
GT/$AgNO_3$ solution		
at 6 h	449 ± 1	1323 ± 1
at 12 h	450 ± 1	1357 ± 1
at 24 h	448 ± 1	1371 ± 1
at 2 d	362 ± 1	1398 ± 1

3.2. Neat and nAg-loaded e-spun gelatin fiber mats

3.2.1. Morphology before and after cross-linking treatment

Fig. 3 shows selected SEM images of e-spun fiber mats from both the base and the 12 h-aged $AgNO_3$-containing gelatin solutions. Only cross-sectionally round fibers, without the presence of beads, were obtained. The diameters of the individual fibers obtained from these solutions were 230 ± 30 and 280 ± 40 nm, respectively. Fig. 4 shows a TEM image of an e-spun fiber from the 12 h-aged $AgNO_3$-containing gelatin solution (see an additional image in Supplementary data). Apparently, nAg were distributed throughout the fibers, with the diameters of these particles being 13 ± 4 nm, which is in accordance with the values observed by AFM. Notwithstanding, it should be emphasized that, at 12 h of aging, silver was present both as Ag^+ ions and as elemental Ag; but for convenience, nAg was used loosely to denote both forms of silver that were present in the e-spun fiber. Quantitative assessment by EDX of the amount of the elemental Ag in the e-spun fiber mat from the 12 h-aged $AgNO_3$-containing gelatin solution indicated a value of 0.26 wt%. Note that the EDX pattern of the elemental Ag observed in this fiber mat sample, including a summary of all of the detectable elements, is available as Supplementary data.

Since gelatin is water-soluble, an e-spun gelatin fiber mat can easily dissolve either partially or completely, losing its fibrous structure when coming into contact with an aqueous medium. It may partially dissolve and lose its fibrous structure upon exposure to high ambient humidity (e.g., 80–90%) for a certain period of time [28]. To extend the use of e-spun gelatin fiber mats in applications that require exposure to an aqueous medium or high humidity, further cross-linking is necessary. Among the various chemical systems used to cross-link an e-spun gelatin fiber mat (e.g., HDMI [24], EDC [25], and GTA vapor [27,28]), GTA is seemingly the most suitable, as it is economical and does not compromise the fibrous structure of the e-spun membrane. Here, the neat and the nAg-containing e-spun gelatin fiber mats were further cross-linked by saturated vapor from 50 vol% GTA aqueous solution for either 1 or 3 h, followed by a heat treatment at 110 °C for 24 h. Cross-linking treatment did not affect the amount of nAg in the cross-linked e-spun gelatin fiber mats, as the amount was determined by EDX to be about the same at 0.27 wt% (see Supplementary data for the EDX patterns of the elemental Ag observed in these fiber mat samples, including a summary of all of the detectable elements in these samples).

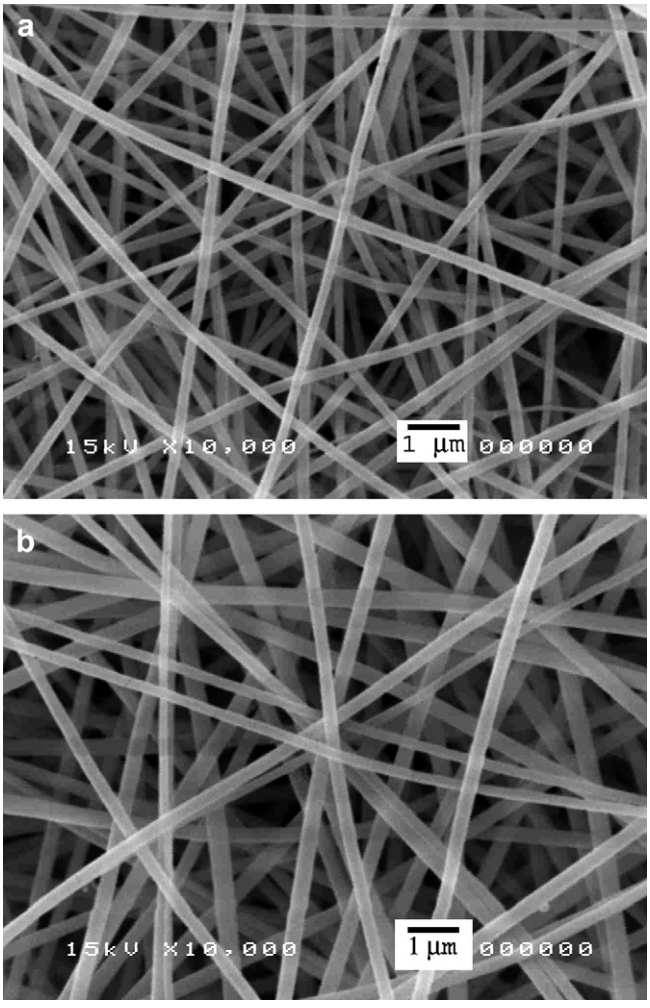

Fig. 3. Selected SEM images of the electrospun fiber mats from (a) the base gelatin solution and (b) the $AgNO_3$-containing gelatin solution that had been aged for 12 h. The diameters of the individual fibers obtained from these solutions were 230 ± 30 and 280 ± 40 nm, respectively.

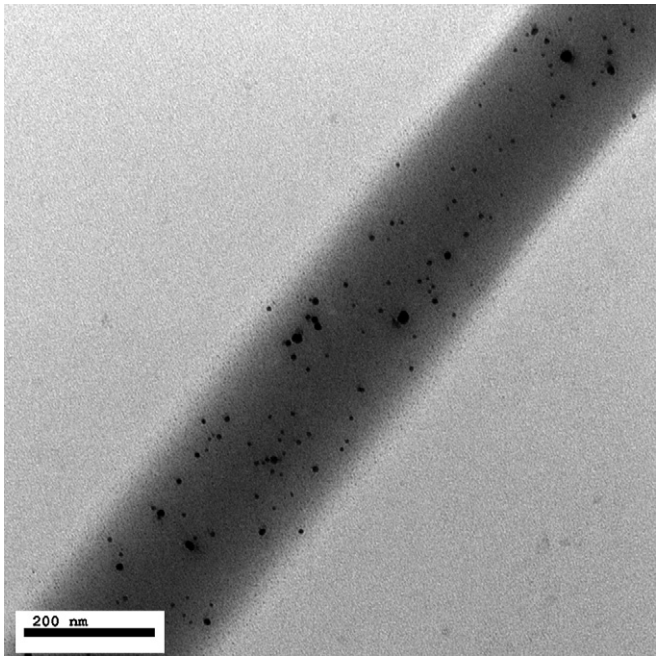

Fig. 4. Selected TEM image of an electrospun fiber from the $AgNO_3$-containing gelatin solution that had been aged for 12 h. The diameters of the as-formed nAg were 13 ± 4 nm.

Fig. 5 shows selected SEM images of the e-spun fiber mats from both the neat and the 12 h-aged $AgNO_3$-containing gelatin solutions after having been cross-linked with moist GTA vapor for either 1 or 3 h. Evidently, exposing the fiber mats in the chamber caused some fibers to fuse to one another at touching points, a result of the partial dissolution of the fiber segments when they came into contact with the moisture-rich GTA vapor. A similar observation was reported for the cross-linking of the e-spun poly(vinyl alcohol) (PVA) fibers containing sodium salicylate as the model drug with moist GTA vapor [45]. In addition, both the neat and the nAg-containing e-spun gelatin fiber mats, after cross-linking, changed their color from white to yellow (for the fiber mats that had been cross-linked for 1 h) and finally to brown (for the fiber mats that had been cross-linked for 3 h). They also shrunk slightly from their original dimensions. The change in color of the gelatin upon cross-linking with GTA is caused by the formation of aldimine linkages (–CH═N–) between the free amino groups of lysine or hydroxylysine amino acid residues of the protein and the aldehyde groups of GTA [46,47]. Moreover, the shrinkage of the fiber mats is responsible for the observed decrease in the size of inter-fibrous

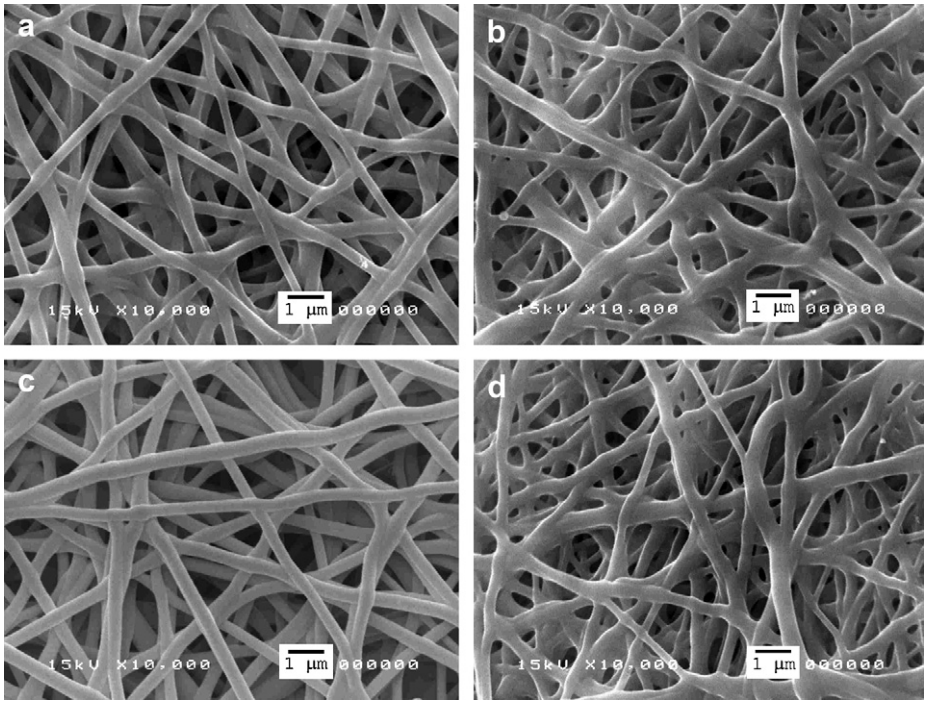

Fig. 5. Morphology of the electrospun fiber mats from (a,b) the base gelatin solution and (c,d) the $AgNO_3$-containing gelatin solution that had been aged for 12 h, after having been cross-linked with moist vapor of glutaraldehyde for (a,c) 1 h or (b,d) 3 h.

pores (cf. SEM images in Figs. 3 and 5), as well as the observed decrease in the thickness of the fiber mats and the observed increase in the diameters of the individual fibers (see Table 2).

3.2.2. Weight loss and water retention behavior

To assess the degree of cross-linking, both the neat and the nAg-containing e-spun gelatin fiber mats that had been cross-linked with moist GTA vapor for either 1 or 3 h were investigated for weight loss and water retention behavior after submersion in distilled water, acetate buffer, or SBF for various submersion time intervals (1, 2 and 7 d). The results of such analyses are available as Supplementary data. For a given exposure time in the cross-linking chamber and a given type of medium, the weight loss and water retention ability for both types of e-spun gelatin fiber mats increased with an increase in submersion time. As expected, an increase in the exposure time of the fiber mat samples in the cross-linking chamber caused both the weight loss and the water retention ability of the samples to decrease, a result of the increase in the extent of cross-linking with increasing exposure time. For any given submersion time, both the weight loss and the water retention of the fiber mat samples was greatest when they were submerged in SBF, followed by those in distilled water and acetate buffer, respectively. The actual reason for such behavior is not known, but it is postulated to be a result of the various ions that are present in SBF.

3.2.3. Thermal and mechanical integrity

Fig. 6 shows TGA thermograms of both the neat and the nAg-containing e-spun gelatin fiber mats that had been cross-linked for either 1 or 3 h. For all of the fiber mat samples, two stages in the loss of their weight were observed. The first stage should correspond to the loss of moisture from these samples, while the second one should be due to the thermal decomposition of gelatin. The loss of moisture in these samples occurred over a temperature range of 25 to ~90 to ~150 °C. The moisture content in these samples ranged between ~9 and ~14%, with the values for the uncross-linked ones being the greatest (i.e., at ~14% for the neat gelatin fiber mat samples and ~12% for the nAg-containing counterparts). The onset value for the thermal decomposition ($T_{d,onset}$) of the uncross-linked, neat gelatin fiber mat samples occurred at ~269 °C, while a much lower value was observed for the uncross-linked, nAg-containing counterparts (i.e., at ~206 °C). Cross-linking of these fiber mats with moist GTA vapor drastically increased the thermal stability of the materials. Specifically, $T_{d,onset}$ values of the 1- and 3 h-cross-linked gelatin fiber mat samples were ~350 and ~354 °C, while such values for the cross-linked nAg-containing counterparts were ~326 and ~360 °C, respectively. Cross-linking was also responsible for the observed increase in the char contents of the cross-linked materials, as opposed to their uncross-linked counterparts.

The results of the mechanical assessment of both the neat and the nAg-containing e-spun gelatin fiber mats that had been cross-linked for either 1 or 3 h are presented in Table 3. Both the tensile strength and the Young's modulus of the uncross-linked, neat gelatin fiber mat samples were 2.2 and 126.6 MPa, while such values for the uncross-linked, nAg-containing counterparts were slightly lower, at 1.9 and 52.8 MPa. Equivalent values of 1.3 and 46.5 MPa for the uncross-linked, neat gelatin fiber mats were

Table 2
Diameters of the individual fibers and thicknesses of the electrospun fiber mats from the base gelatin (GT) solution and the $AgNO_3$-containing GT solution that had been aged for 12 h, after having been cross-linked with moist vapor of glutaraldehyde for 1 or 3 h

Type of samples	After cross-linking for 1 h		After cross-linking for 3 h	
	Thicknesses of fiber mats (μm)	Diameters of individual fibers (nm)	Thicknesses of fiber mats (μm)	Diameters of individual fibers (nm)
Neat GT fiber mat	230 ± 70	300 ± 50	150 ± 50	380 ± 80
$AgNO_3$-containing GT fiber mat	220 ± 60	360 ± 60	190 ± 20	410 ± 80

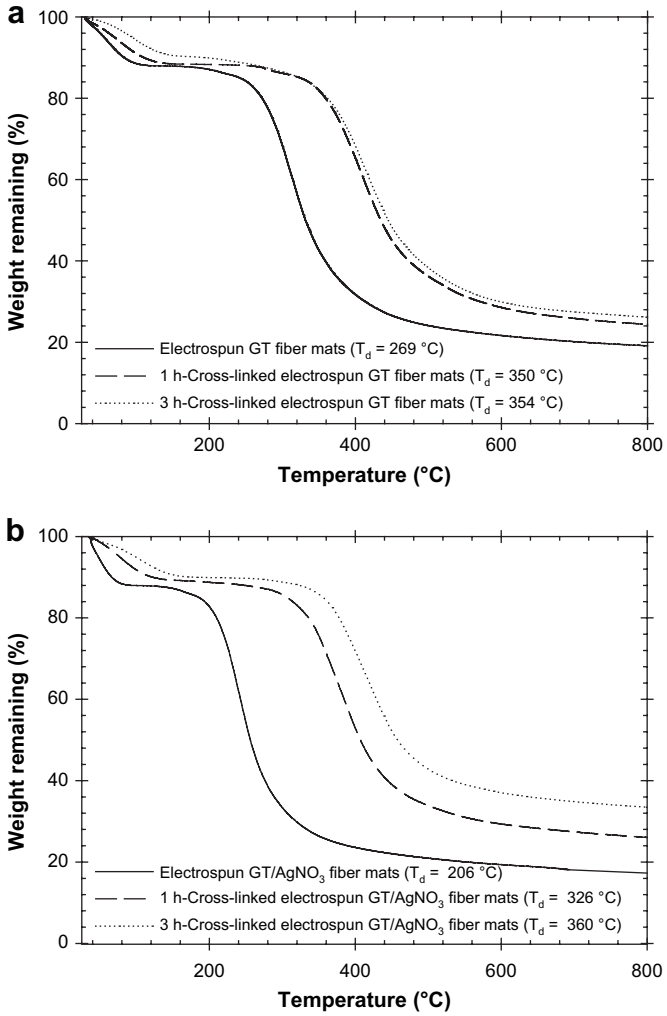

Fig. 6. Thermogravimetric spectra of the electrospun fiber mats from (a) the base gelatin solution and (b) the $AgNO_3$-containing gelatin solution that had been aged for 12 h, after having been cross-linked with moist vapor of glutaraldehyde for 1 or 3 h.

reported by Zhang et al. [28]. Dramatic improvement in both the tensile strength and the Young's modulus of the materials was observed after cross-linking with moist GTA vapor. A similar observation was also reported by Zhang et al. [28]. As shown in Fig. 5 and Table 2, cross-linking of both types of gelatin fiber mats with moist GTA vapor not only caused the diameters of the individual fibers to increase, but also was responsible for the fusing of the fibers at touching points. Lee et al. [48] postulated that the fusing of e-spun fibers of poly(vinyl chloride) (PVC) and polyurethane (PU) with increasing PU content was responsible for the observed improvement in the mechanical integrity of the obtained fiber mats. It is postulated here that both the formed inter- and intra-molecular covalent bonds and the fusing between the fiber junctions should be responsible for the dramatic improvement in both the tensile strength and the Young's modulus of the studied materials [28]. On the contrary, cross-linking caused an adverse effect on the elongation at break of the studied materials, as the property values of the cross-linked fiber mat samples were lower than those of the uncross-linked ones.

Table 3
Mechanical integrity of the electrospun fiber mats from the base gelatin (GT) solution and the 12 h-aged $AgNO_3$-containing GT solution, after having been cross-linked with moist vapor of glutaraldehyde for 1 or 3 h

Cross-linking time (h)	Tensile strength (MPa)	
	Neat GT fiber mat	$AgNO_3$-containing GT fiber mat
0	2.2 ± 0.5	1.9 ± 0.2
1	13.7 ± 6.0	20.3 ± 3.0
3	27.3 ± 7.3	33.6 ± 12.7
Cross-linking time (h)	Young's modulus (MPa)	
	Neat GT fiber mat	$AgNO_3$-containing GT fiber mat
0	126.6 ± 90.5	52.8 ± 17.1
1	996.3 ± 414.2	1090.7 ± 120.4
3	1025.9 ± 171.2	1171.0 ± 353.7
Cross-linking time (h)	Elongation at break (%)	
	Neat GT fiber mat	$AgNO_3$-containing GT fiber mat
0	13.6 ± 2.6	9.8 ± 2.1
1	8.2 ± 1.5	5.8 ± 1.1
3	6.6 ± 2.5	4.7 ± 1.4

3.2.4. Release characteristic of silver

Prior to investigating the release characteristic of silver from the nAg-containing e-spun gelatin fiber mats that had been cross-linked for 1 or 3 h, the actual amount and the form of silver that was released from the materials needed to be identified. To determine the amount of silver in these samples, the uncross-linked fiber mat specimens which had been prepared from the gelatin solution containing 2.5 wt% $AgNO_3$ (corresponding to the theoretical content of the as-loaded Ag^+ of ca. 15.49 mg/g of the fiber mats) were first dissolved in 5 mL of 95% HNO_3, followed by the addition of an appropriate releasing medium (i.e., acetate buffer, distilled water, or SBF) to attain the final volume of 50 mL. The obtained silver-containing solutions in such media were then determined for the actual content of as-loaded silver (by means of AAS) to be 15.11 ± 0.45, 15.12 ± 1.33, and 15.01 ± 0.21 mg/g of the fiber mats. This accounted for 97.6 ± 2.9, 97.7 ± 8.6, and 96.9 ± 1.3% of the initial, theoretical content of the as-loaded Ag^+. On the other hand, the sample solution containing silver that was released from the 1 h-cross-linked nAg-containing e-spun gelatin fiber mat specimen that had been submerged in acetate buffer for 7 d was used as a model system to verify whether the as-released silver was in the form of Ag^+ ions. This was done by direct titration with a NaCl solution. Though not shown, the obtained result confirmed that the as-released silver was in the form of Ag^+ ions.

Prior to further investigation for the release characteristic of Ag^+ ions from these materials, it should be emphasized that these nAg-containing fibrous materials were prepared from the gelatin solution containing 2.5 wt% $AgNO_3$ that had been aged for 12 h prior to e-spinning. At 12 h of aging, silver was present both in ionic and metallic nanoparticle forms, as previously discussed. At 2.5 wt% of $AgNO_3$ that was loaded in the gelatin solution, the theoretical amount of the as-loaded Ag^+ in the obtained fiber mats should be ca. 15.49 mg/g of the fiber mats. Some of these ions were reduced into elemental Ag upon aging. Evidently, the amounts of both the remnant Ag^+ ions (the ones that remained in the ionic form) and the Ag^+ ions that resulted from the dissolution of the as-formed elemental Ag^0 constituted ca. 15.01–15.12 mg/g of the fiber mats, or ca. 96.9–97.7% of the initial amount of Ag^+ loaded in the gelatin solution. As proven by the titration method as well as by visual observation of the sample solution containing silver that was released from the 1 h-cross-linked nAg-containing e-spun gelatin fiber mat specimen that had been submerged in acetate buffer for 7 d, only silver in the ionic form was released. Pal [49] showed that, in an aqueous medium containing a nucleophile (e.g., $NaBH_4$, SCH^-, and I^-), the dissolution of silver is possible due to a significant decrease in the reduction potential. The redox reaction for silver dissolution can be written as:

$$4Ag + O_2 + 2H_2O \leftrightarrow 4Ag^+ + 4OH^-. \quad (3)$$

Here, it is postulated that the as-formed nAg dissolved readily upon contact with the releasing medium, and that both the remnant and

the dissolved Ag^+ ions were released into the medium during the release studies.

The release characteristic of Ag^+ ions from either the 1 h or the 3 h-cross-linked nAg-containing e-spun gelatin fiber mat samples was investigated by the total immersion method in one of the releasing media (i.e., the acetate buffer, distilled water, and SBF). The cumulative amount of Ag^+ ions released from these materials is reported in Fig. 7 as the weight of Ag^+ ions released (in mg) divided by the weight of the specimens (in g). Evidently, the cumulative amount of Ag^+ ions released from the samples in the acetate buffer and distilled water occurred rather rapidly during the first 60 min after submersion in the releasing medium, and then increased gradually afterwards. For 1 h-cross-linked nAg-containing e-spun gelatin fiber mat specimens, the cumulative amount of Ag^+ ions released from the specimens in distilled water was greater than that released in the acetate buffer during the first 6 h of submersion, while that released from specimens in the acetate buffer was increasingly greater afterwards. A similar trend was observed for the 3 h-cross-linked nAg-containing e-spun gelatin fiber mat specimens, in which the cumulative amount of Ag^+ ions released from these specimens in distilled water was greater than the amount released in the acetate buffer during the first 30 min of submersion.

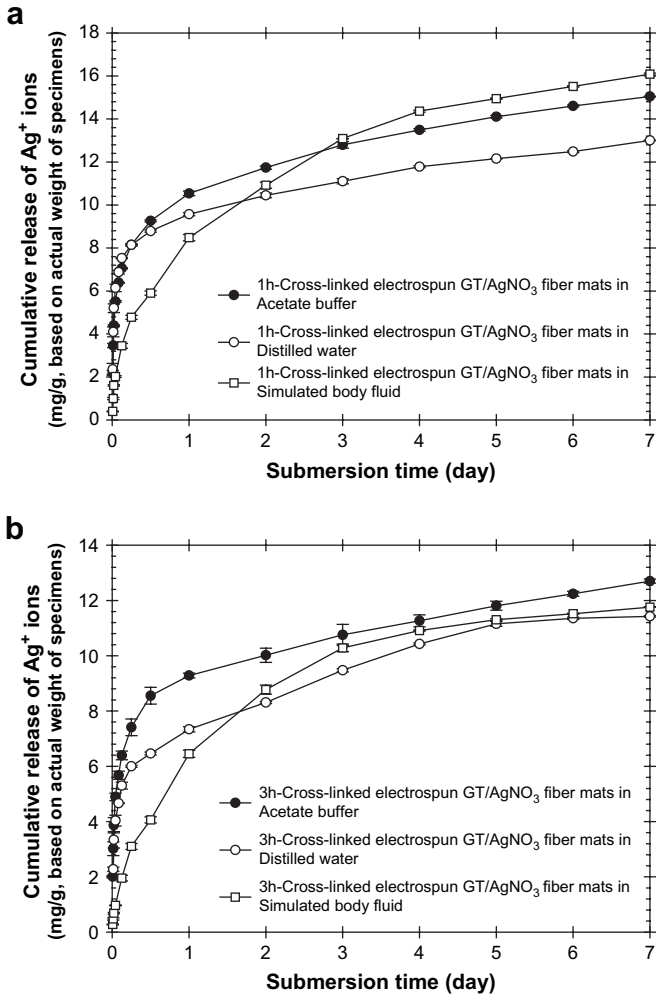

Fig. 7. Cumulative release profiles of Ag^+ ions from 1- and 3 h-cross-linked nAg-containing e-spun gelatin (GT) fiber mat specimens reported as the weight of Ag^+ ions released (in mg) divided by the actual weight of specimens (in g) in three types of releasing medium, i.e., (a) acetate buffer (pH 5.5), (b) distilled water (pH 6.9), at the skin temperature of 32 °C, and (c) simulated body fluid (pH 7.4), at the physiological temperature of 37 °C.

On the other hand, a significantly different releasing characteristic of Ag^+ ions from either the 1- or the 3 h-cross-linked nAg-containing e-spun gelatin fiber mat samples was evident in the case where SBF was the releasing medium. The cumulative amount of Ag^+ ions released in SBF occurred more gradually over the testing period. For 1 h-cross-linked nAg-containing e-spun gelatin fiber mat specimens, the cumulative amount of Ag^+ ions released from these specimens in SBF was lower than the amounts released in both the acetate buffer and distilled water during the first 2 and 3 d of submersion, while it was increasingly greater afterwards. While the initially lower amount of Ag^+ ions released in SBF could be due to the neutralization effect of various anions (especially Cl^-) that are present in the medium, the greater amount of Ag^+ ions released at later submersion times could be due to the observed greater values of weight loss and water retention of these samples in SBF than in the other two media. For 3 h-cross-linked nAg-containing e-spun gelatin fiber mat specimens, the cumulative amount of Ag^+ ions released from the specimens in SBF was greater only than the amount released in distilled water after ~2 d of submersion, while it was lower than the amount released in acetate buffer for all submersion periods.

Between the two sample types, the cumulative amount of Ag^+ ions released from the 1 h-cross-linked nAg-containing e-spun gelatin fiber mat specimens in any type of releasing medium was systematically greater than the amount released from the 3 h-cross-linked ones. This is possibly a result of the observed lower weight loss and water retention of the 3 h-cross-linked nAg-containing e-spun gelatin fiber mat specimens in comparison with those of their 1 h-cross-linked counterparts.

Quantitatively, the cumulative amount of Ag^+ ions released from the 1 h-cross-linked nAg-containing e-spun gelatin fiber mat specimens in the acetate buffer increased from ~5.5 mg/g of the specimens at 60 min, to attain a final value of ~15.0 mg/g of the specimens at day 7. For the 3 h-cross-linked nAg-containing e-spun gelatin fiber mat specimens, the amount of Ag^+ ions increased from ~4.9 mg/g of the specimens at 60 min to ~12.7 mg/g of the specimens at day 7. In distilled water, the cumulative amount of Ag^+ ions released from the 1 h-cross-linked nAg-containing e-spun gelatin fiber mat specimens increased from ~6.1 mg/g of the specimens at 60 min to ~13.0 mg/g of the specimens at day 7. For the 3 h-cross-linked nAg-containing e-spun gelatin fiber mat specimens, it increased from ~4.7 mg/g of the specimens at 60 min to ~11.5 mg/g of the specimens at day 7. In SBF, the cumulative amount of Ag^+ ions released from the 1 h-cross-linked nAg-containing e-spun gelatin fiber mat specimens increased from ~2.0 mg/g of the specimens at 60 min to ~16.1 mg/g of the specimens at day 7. For the 3 h-cross-linked nAg-containing e-spun gelatin fiber mat specimens, it increased from ~1.0 mg/g of the specimens at 60 min to ~11.8 mg/g of the specimens at day 7. The possible reason for the observed greater release of Ag^+ ions from both types of samples in acetate buffer than in distilled water could be due to the protonation of the amino groups of gelatin. The pH value of the buffer medium was supposedly less than the isoelectric point (PI) of the type-A gelatin (i.e., PI ≈ 7–9) used in this work [50]; while the amount of Ag^+ ions released from the 1 h-cross-linked nAg-containing e-spun gelatin fiber mat specimens – greater in SBF than in the other two media – should be due to the observed greater values of weight loss and water retention in the medium.

Alternatively, the cumulative amount of Ag^+ ions released from these materials can also be reported as the concentration of the as-released Ag^+ ions in the releasing media (i.e., in ppm or mg/L of the releasing media) divided by the actual weight of the specimens (in g); and as the percentage of the weight of the as-released Ag^+ ions divided by the actual weight of Ag^+ ions in the specimens (see Supplementary data). The cumulative releasing profiles of Ag^+ ions from these samples in any type of releasing medium were similar to

Table 4
Antibacterial activity of the electrospun fiber mats from the base gelatin (GT) solution and the 12 h-aged $AgNO_3$-containing GT solution, after having been cross-linked with moist vapor of glutaraldehyde for 1 or 3 h with or without washing with glycine, against some common bacteria found on burn wounds

Type of samples	Antibacterial activity in terms of disc diffusion method reported as inhibition zone diameter (cm)/sample diameter (cm)			
	E. coli 25922	*P. aeroginosa* 27853	*S. aureus* 25023	Methicillin-resistant *S. aureus* 20627
Neat GT fiber mat				
1 h-cross-linking w/o glycine washing	1.60/1.60	1.50/1.50	1.50/1.50	1.50/1.50
1 h-cross-linking w/glycine washing	1.60/1.60	1.50/1.50	1.50/1.50	1.50/1.50
3 h-cross-linking w/o glycine washing	1.65/1.65	1.50/1.50	1.50/1.50	1.50/1.50
3 h-cross-linking w/glycine washing	1.50/1.50	1.50/1.50	1.50/1.50	1.60/1.60
$AgNO_3$-containing GT fiber mat				
1 h-cross-linking w/o glycine washing	2.00/1.50	2.20/1.60	2.40/1.50	1.87/1.50
1 h-cross-linking w/glycine washing	2.07/1.60	2.43/1.60	2.43/1.50	2.03/1.60
3 h-cross-linking w/o glycine washing	1.77/1.50	2.37/1.60	2.43/1.60	2.17/1.60
3 h-cross-linking w/glycine washing	2.20/1.60	2.47/1.50	2.27/1.60	1.93/1.60

Note: The zone of inhibition of Gentamycin disc against *E. coli* and *P. aeroginosa* was 2.60 and 1.83 cm, respectively, and the zone of inhibition of Vancomycin disc against *S. aureus* and MRSA was 1.83 and 1.93 cm, respectively.

those shown in Fig. 7. Based on the actual weight of the as-loaded Ag^+ ions in these samples, ~99, ~85 and ~107% of Ag^+ ions were released from the 1 h-cross-linked nAg-containing e-spun gelatin fiber mat specimens in the acetate buffer, distilled water, and SBF, respectively; while ~82, ~76 and ~78% of the ions were released from their 3 h-cross-linked counterparts.

3.2.5. Antimicrobial activity

The potential for use of nAg-containing e-spun gelatin fiber mats as functional wound dressings was assessed by observing their antibacterial activity (based on the disc diffusion method) against some common bacteria found on burn wounds: *E. coli*, *P. aeroginosa*, *S. aureus* and MRSA. The activity of the neat e-spun gelatin fiber mats against these bacteria was used as a control. Since both the neat and the nAg-containing e-spun gelatin fiber mat specimens were cross-linked with GTA vapor to enhance their stability in an aqueous medium, the effect of glycine treatment to neutralize unreacted aldehyde groups of GTA [51] on the antibacterial activity of the glycine-treated specimens was also investigated. The results of such studies are available as Supplementary data. Both the diameters of the inhibition zone and those of the specimens were analyzed accordingly; the results are reported in Table 4. It should be noted that the initial diameter of all the specimens was fixed at 1.5 cm. However, in a wet condition, the specimens swelled, resulting in the observed dimensional change. If the specimens swelled appreciably prior to deposition on the agar plate, the final, not the initial, diameter of the specimens was reported.

According to the results obtained, all of the cross-linked neat e-spun gelatin fiber mat specimens, with or without glycine treatment, showed no activity against the tested bacteria. For the nAg-containing specimens, inhibitory zones were evident. Specifically, the antibacterial activity of the nAg-containing specimens, regardless of the sample type, was greatest against *P. aeroginosa*, followed by *S. aureus*, *E. coli* and MRSA, respectively. Without glycine washing, the nAg-containing specimens were more effective against *S. aureus* and MRSA; with glycine washing, they were more effective in inhibiting *E. coli* and *P. aeroginosa*. The reason for such an observation is not certain at this point. Feng et al. [52] demonstrated that, upon interacting with Ag^+ ions, both *E. coli* and *S. aureus* underwent a series of events that led to their demise. Specifically, they postulated that the bactericidal mechanism was based on the ability of Ag^+ ions to bind with certain chemical functionalities of the cell wall, the cytoplasm and the nucleus. This causes DNA molecules to condense, the cytoplasmic membrane to detach from the cell wall, and the cell wall to become severely damaged [52]. A similar observation of the bactericidal effect of nAg and/or Ag^+ ions has been reported [53,54].

4. Conclusion

Silver ions (Ag^+ ions), known for their broad-spectrum antimicrobial activity, were reduced into silver nanoparticles (nAg) in a base gelatin (type A, porcine skin, 170-190 Bloom) solution (22% w/v in 70 vol% acetic acid) containing 2.5 wt% $AgNO_3$ (based on the weight of the gelatin powder). The presence of nAg in the $AgNO_3$-containing gelatin solution was first realized after it had been aged for at least 12 h. The amount of nAg formed increased monotonically with increasing aging time. The average diameters of the as-formed nAg ranged between ~11 and ~20 nm. Both the base and the 12 h-aged $AgNO_3$-containing gelatin solutions were fabricated into ultrafine fibers by electrospinning (15 kV/20 cm). The average diameters of these fibers were ~230 and ~280 nm, respectively, with the average diameter of the as-formed nAg in the electrospun (e-spun) fibers from the 12 h-aged $AgNO_3$-containing gelatin solution being ~13 nm. Both the neat and the nAg-containing gelatin fiber mats were further cross-linked, to improve their stability in an aqueous medium or a high humidity atmosphere, by saturated vapor from 50 vol% glutaraldehyde (GTA) aqueous solution, followed by a heat treatment at 110 °C for 24 h. Cross-linking not only caused the color of the cross-linked gelatin fibers to change, but also was responsible for the fusing and shrinking of the cross-linked fiber mats. Weight loss and water retention of both the neat and the nAg-containing gelatin fiber mats in acetate buffer (pH 5.5), distilled water (pH 6.9) and simulated body fluid (SBF; pH 7.4) were found to decrease with increasing exposure time in the cross-linking chamber. The release characteristic of Ag^+ ions from either the 1 or the 3 h-cross-linked nAg-containing e-spun gelatin fiber mats was investigated by the total immersion method in acetate buffer, distilled water (both at skin temperature of 32 °C), and SBF (at the physiological temperature of 37 °C). The cumulative release of Ag^+ ions from the samples in the acetate buffer and distilled water occurred rather rapidly during the first 60 min after submersion in the releasing medium, and increased gradually afterwards; while those in SBF occurred more gradually over the testing period. Lastly, the antibacterial activity of these materials (with or without glycine washing, regardless of the sample types) was greatest against *P. aeroginosa*, followed by *S. aureus*, *E. coli*, and methicillin-resistant *S. aureus*, respectively.

Acknowledgments

The authors acknowledge partial support received from the National Nanotechnology Center (grant number: BR0108); the National Center of Excellence for Petroleum, Petrochemicals, and Advanced Materials (NCE-PPAM); and the Petroleum and Petrochemical College (PPC), Chulalongkorn University. PR

acknowledges a doctoral scholarship received from the Thailand Graduate Institute of Science and Technology (TGIST) (TG-55-09-49-067D).

Appendix. Supplementary data

Supplementary data associated with this article can be found in the online version, at doi:10.1016/j.polymer.2008.08.021.

References

[1] Reneker DH, Yarin AL. Electrospinning jets and polymer nanofibers. Polymer 2008;49:2387–425.
[2] Shim YM, Hohman MM, Brenner MP, Rutledge GC. Experimental characterization of electrospinning: the electrically forced jet and instabilities. Polymer 2001;42:9955–67.
[3] Ding B, Kim HY, Lee SC, Shao CL, Lee DR, Park SJ, et al. Preparation and characterization of a nanoscale poly(vinyl alcohol) fiber aggregate produced by an electrospinning method. J Polym Sci Part B Polym Phys 2002;40:1261–8.
[4] Wu LL, Yuan XY, Sheng J. Immobilization of cellulase in nanofibrous PVA membranes by electrospinning. J Membr Sci 2005;250:167–73.
[5] Choi JS, Lee SW, Jeong L, Bae SH, Min BC, Youk JH, et al. Effect of organosoluble salts on the nanofibrous structure of electrospun poly(3-hydroxybutyrate-*co*-3-hydroxyvalerate). Int J Biol Macromol 2004;34:249–56.
[6] Kim K, Luu YK, Chang C, Fang DF, Hsiao BS, Chu B, et al. Incorporation and controlled release of a hydrophilic antibiotic using poly(lactide-*co*-glycolide)-based electrospun nanofibrous scaffolds. J Controlled Release 2004;98:47–56.
[7] Luu YK, Kim K, Hsiao BS, Chu B, Hadjiargyrou M. Development of a nanostructured DNA delivery scaffold via electrospinning of PLGA and PLA–PEG block copolymers. J Controlled Release 2003;89:341–53.
[8] Kenawy ER, Bowlin GL, Mansfield K, Layman J, Simpson DG, Sanders EH, et al. Release of tetracycline hydrochloride from electrospun poly(ethylene-*co*-vinylacetate), poly(lactic acid), and a blend. J Controlled Release 2002;81:57–64.
[9] Zong XH, Kim K, Fang DF, Ran SF, Hsiao BS, Chu B. Structure and process relationship of electrospun bioabsorbable nanofiber membranes. Polymer 2002;43:4403–12.
[10] Zeng J, Xu X, Chen X, Liang Q, Bian X, Yang L, et al. Biodegradable electrospun fibers for drug delivery. J Controlled Release 2003;92:227–31.
[11] Verreck G, Chun I, Peeters J, Rosenblatt J, Brewster ME. Preparation and characterization of nanofibers containing amorphous drug dispersions generated by electrostatic spinning. Pharm Res 2003;20:810–7.
[12] Verreck G, Chun I, Rosenblatt J, Peeters J, van Dijck A, Mensch J, et al. Incorporation of drugs in an amorphous state into electrospun nanofibers composed of a water-insoluble, nonbiodegradable polymer. J Controlled Release 2003;92:349–60.
[13] Young S, Wong M, Tabata Y, Mikos AG. Gelatin as a delivery vehicle for the-controlled release of bioactive molecules. J Controlled Release 2005;109:256–74.
[14] Jongjareonrak A, Benjakul S, Visessanguan W, Prodpran T, Tanaka M. Characterization of edible films from skin gelatin of brownstripe red snapper and bigeye snapper. Food Hydrocolloids 2006;20:492–501.
[15] Huss FRM, Junker JPE, Johnson H, Kratz G. Macroporous gelatine spheres as culture substrate, transplantation vehicle, and biodegradable scaffold for guided regeneration of soft tissues. In vivo study in nude mice. J Plast Reconstr Aesthet Surg 2007;60:543–55.
[16] Vandervoort J, Ludwig A. Preparation and evaluation of drug-loaded gelatin nanoparticles for topical ophthalmic use. Eur J Pharm Biopharm 2004;57:251–61.
[17] Tabata Y, Hijikata S, Ikada Y. Enhanced vascularization and tissue granulation by basic fibroblast growth factor impregnated in gelatin hydrogels. J Controlled Release 1994;31:189–99.
[18] Liu TY, Hu SH, Liu KH, Liu DM, Chen SY. Preparation and characterization of smart magnetic hydrogels and its use for drug release. J Magn Magn Mater 2006;304:e397–9.
[19] Liu J, Meisner D, Kwong E, Wu XY, Johnston MR. A novel trans-lymphatic drug delivery system: implantable gelatin sponge impregnated with PLGA–paclitaxel microspheres. Biomaterials 2007;28:3236–44.
[20] Fukae R, Maekawa A, Sangen O. Gel-spinning and drawing of gelatin. Polymer 2005;46:11193–4.
[21] Huang ZM, Zhang YZ, Ramakrishna S, Lim CT. Electrospinning and mechanical characterization of gelatin nanofibers. Polymer 2004;45:5361–8.
[22] Zhang Y, Ouyang H, Lim CT, Ramakrishna S, Huang ZM. Electrospinning of gelatin fibers and gelatin/PCL composite fibrous scaffolds. J Biomed Mater Res Appl Biomater 2005;72B:156–65.
[23] Ki CS, Baek DH, Gang KD, Lee KH, Um IC, Park YH. Characterization of gelatin nanofiber prepared from gelatin–formic acid solution. Polymer 2005;46:5094–102.
[24] Li M, Mondrinos MJ, Gandhi MR, Ko FK, Weiss AS, Lelkes PI. Electrospun protein fibers as matrices for tissue engineering. Biomaterials 2005;26:5999–6008.
[25] Li M, Guo Y, Wei Y, MacDiarmid AG, Lelkes PI. Electrospinning polyaniline-contained gelatin nanofibers for tissue engineering applications. Biomaterials 2006;27:2705–15.
[26] Choktaweesap N, Arayanarakul K, Aht-ong D, Meechaisue C, Supaphol P. Electrospun gelatin fibers: effect of solvent system on morphology and fiber diameters. Polym J 2007;39:622–31.
[27] Songchotikunpan P, Tattiyakul J, Supaphol P. Extraction and electrospinning of gelatin from fish skin. Int J Biol Macromol 2008;42:247–55.
[28] Zhang YZ, Venugopal J, Huang ZM, Lim CT, Ramakrishna S. Crosslinking of the electrospun gelatin nanofibers. Polymer 2006;47:2911–7.
[29] Sikareepaisan P, Suksamrarn A, Supaphol P. Electrospun gelatin fiber mats containing a herbal – *Centella asiatica* – extract and release characteristic of asiaticoside. Nanotechnology 2007;19:015102 (10 pp).
[30] Wright JB, Lam K, Buret AG, Olson ME, Burrell RE. Early healing events in a porcine model of contaminated wounds: effects of nanocrystalline silver on matrix metalloproteinases, cell apoptosis, and healing. Wound Repair Regen 2002;10:141–51.
[31] Jones SA, Bowler PG, Walker M, Parsons D. Controlling wound bioburden with a novel silver-containing Hydrofiber® dressing. Wound Repair Regen 2004;12:288–94.
[32] Gallant-Behm CL, Yin HQ, Jui S, Heggers JP, Langford RE, Olson M, et al. Comparison of in vitro disc diffusion and time kill-kinetic assays for the evaluation of antimicrobial wound dressing efficacy. Wound Repair Regen 2005;13:412–21.
[33] Leaper DJ. Silver dressings: their role in wound management. Int Wound J 2006;3:282–94.
[34] Field CK, Kerstein MD. Overview of wound healing in a moist environment. Am J Surg 1994;167:s2–6.
[35] Yang QB, Li DM, Hong YL, Li ZY, Wang C, Qiu SL, et al. Preparation and characterization of a PAN nanofibre containing Ag nanoparticles via electrospinning. Synth Met 2003;137:973–4.
[36] Lee HK, Jeong EH, Baek CK, Youk JH. One-step preparation of ultrafine poly(acrylonitrile) fibers containing silver nanoparticles. Mater Lett 2005;59:2977–80.
[37] Lim SK, Lee SK, Hwang SH, Kim H. Photocatalytic deposition of silver nanoparticles onto organic/inorganic composite nanofibers. Macromol Mater Eng 2006;291:1265–70.
[38] Son WK, Youk JH, Lee, Park WH. Preparation of antimicrobial ultrafine cellulose acetate fibers with silver nanoparticles. Macromol Rapid Commun 2004;25:1632–7.
[39] Son WK, Youk JH, Park WH. Antimicrobial cellulose acetate nanofibers containing silver nanoparticles. Carbohydr Polym 2006;65:430–4.
[40] Jin WJ, Lee HK, Jeong EH, Park WH, Youk JH. Preparation of polymer nanofibers containing silver nanoparticles by using poly(*N*-vinylpyrrolidone). Macromol Rapid Commun 2005;26:1903–7.
[41] Hong KH, Park JL, Sul IH, Youk JH, Kang TJ. Preparation of antimicrobial poly(vinyl alcohol) nanofibers containing silver nanoparticles. J Polym Sci Part B Polym Phys 2006;44:2468–74.
[42] Hong KH. Preparation and properties of electrospun poly(vinyl alcohol)/silver fiber web as wound dressings. Polym Eng Sci 2007;47:43–9.
[43] Yakutik IM, Shevchenko GP. Self-organization of silver nanoparticles forming on chemical reduction to give monodisperse spheres. Surf Sci 2004;566–568:414–8.
[44] Yiwei A, Yunxia Y, Shuanglong Y, Lihua D, Guorong D. Preparation of spherical silver particles for solar cell electronic paste with gelatin protection. Mater Chem Phys 2007;104:158–61.
[45] Taepaiboon P, Rungsardthong U, Supaphol P. Effect of cross-linking on properties and release characteristics of sodium salicylate-loaded electrospun poly(vinyl alcohol) fiber mats. Nanotechnology 2007;18:175102 (11pp).
[46] Olde Damink LHH, Dijkstra PJ, van Luyn MJA, van Wachem PB, Nieuwenhuis P, Feijen J. Glutaraldehyde as a crosslinking agent for collagen-based biomaterials. J Mater Sci Mater Med 1995;6:460–72.
[47] Akin H, Hasirci N. Preparation and characterization of crosslinked gelatin microspheres. J Appl Polym Sci 1995;58:95–100.
[48] Lee KH, Kim HY, Ryu HJ, Kim KW, Choi SW. Mechanical behavior of electrospun fiber mats of poly(vinyl chloride)/polyurethane polyblends. J Polym Sci Part B Polym Phys 2003;41:1256–62.
[49] Pal T. Nucleophile-induced dissolution of gold and silver in micelle. Curr Sci 2002;83:627–8.
[50] Yang D, Li Y, Nie J. Preparation of gelatin/PVA nanofibers and their potential application in controlled release of drugs. Carbohydr Polym 2007;69:538–43.
[51] Rho KS, Jeong L, Lee G, Seo BM, Park YJ, Hong SD, et al. Electrospinning of collagen nanofibers: effects on the behavior of normal human keratinocytes and early-stage wound healing. Biomaterials 2006;27:1452–61.
[52] Feng QL, Wu J, Chen GQ, Cui FZ, Kim TN, Kim JO. A mechanistic study of the antibacterial effect of silver ions on *Escherichia coli* and *Staphylococcus aureus*. J Biomed Mater Res 2000;52:662–8.
[53] Morones JR, Elechiguerra JL, Camacho A, Holt K, Kouri JB, Ramírez JT, et al. The bactericidal effect of silver nanoparticles. Nanotechnology 2005;16:2346–53.
[54] Shrivastava S, Bera T, Roy A, Singh G, Ramachandrarao P, Dash D. Characterization of enhanced antibacterial effects of novel silver nanoparticles. Nanotechnology 2007;18:225103 (9 pp).